Gene Expression, Vol. 19, pp. 37–47
Printed in the USA.

1052-2166/19 $90.00 + .00
DOI: https://doi.org/10.3727/105221618X15305531034617
E-ISSN 1555-3884
www.cognizantcommunication.com

Heat Stress and Thermal Ablation Induce Local Expression of Nerve Growth Factor Inducible (VGF) in Hepatocytes and Hepatocellular Carcinoma: Preclinical and Clinical Studies

Scott M. Thompson,* Danielle E. Jondal,* Kim A. Butters,* Bruce E. Knudsen,* Jill L. Anderson,* Lewis R. Roberts,† Matthew R. Callstrom,* and David A. Woodrum*

*Department of Radiology, Mayo Clinic School of Medicine, Mayo Clinic, Rochester, MN, USA
†Division of Gastroenterology and Hepatology, Mayo Clinic School of Medicine, Mayo Clinic, Rochester, MN, USA

The purposes of this study were to test the hypothesis that heat stress and hepatic thermal ablation induce nerve growth factor inducible (VGF) and to determine intrahepatic versus systemic VGF expression induced by thermal ablation in vivo and in patients. Hepatocytes and HCC cells were subjected to moderate (45°C) or physiologic (37°C) heat stress for 10 min and assessed for VGF expression at 0–72 h post-heat stress (n 3 experiments). Orthotopic N1S1 HCC-bearing rats were randomized to sham or laser thermal ablation (3 W 90 s), and liver/serum was harvested at 0–7 days postablation for analysis of VGF expression (n 6 per group). Serum was collected from patients undergoing thermal ablation for HCC ($n = 16$) at baseline, 3–6, and 18–24 h postablation and analyzed for VGF expression. Data were analyzed using ordinary or repeated-measures one-way analysis of variance and post hoc pairwise comparison with Dunnett's test. Moderate heat stress induced time-dependent VGF mRNA (3- to 15-fold; $p < 0.04$) and protein expression and secretion (3.1- to 3.3-fold; $p < 0.05$). Thermal ablation induced VGF expression at the hepatic ablation margin at 1 and 3 days postablation but not remote from the ablation zone or distant intrahepatic lobe. There was no detectable serum VGF following hepatic thermal ablation in rats and no increase in serum VGF following HCC thermal ablation in patients at 3–6 and 18–24 h postablation compared to baseline (0.71- and 0.63-fold; $p = 0.27$ and $p = 0.16$, respectively). Moderate heat stress induces expression and secretion of VGF in HCC cells and hepatocytes in vitro, and thermal ablation induces local intrahepatic but not distant intrahepatic or systemic VGF expression in vivo.

Key words: Heat stress; Thermal ablation; Nerve growth factor inducible (VGF); Hepatocellular carcinoma (HCC)

INTRODUCTION

Image-guided, percutaneous thermal ablative therapies are important, minimally invasive treatment options for patients with early stage hepatocellular carcinoma (HCC)[1]. However, aggressive intrasegmental HCC recurrence has been reported in 4%–15% of patients undergoing thermal ablation depending on tumor location and is a negative prognostic factor[2–6]. Recent preclinical studies have shown that moderate heat stress (45°C 10 min) of HCC cells and hepatocytes induces accelerated proliferation of non-heat stressed HCC cells in an in vitro coculture model and that hepatic radiofrequency and laser ablation induce HCC tumor growth in biologically diverse mouse and rat HCC models in vivo[7,8]. Of note, hepatic thermal ablation was shown to induce accelerated local intrahepatic but not distant intrahepatic HCC tumor growth in an energy dose-dependent manner[8]. As such, these data suggest that the degree of heat stress, ablation energy, and proximity of residual HCC within the heat stress or ablation microenvironment may be variables in mediating growth of non-heat stressed HCC cells in vitro or HCC growth in vivo.

Several biological mechanisms have been identified as potential mediators of heat stress, and thermal ablation induced HCC tumorigenesis including inflammatory mediators cyclooxygenase-2 (COX-2), interleukin-6 (IL-6), and signal transducer and activator of transcription 3 (STAT-3), and phosphoinositide 3-kinase/mammalian target of rapamycin/protein kinase B (PI3K/mTOR/AKT) signaling and growth factors including hepatocyte (HGF/c-MET) and epidermal growth factors[7–13]. Moreover, studies have identified several growth factors whose

Address correspondence to Scott M. Thompson, M.D., Ph.D., Department of Radiology, Mayo Clinic, 200 First Street Southwest, Rochester, MN 55905, USA. Tel: (507) 250-3902; Fax: (507) 255-7872; E-mail: thompson.scott@mayo.edu

mRNA expression is induced by moderate heat stress in both HCC cells and hepatocytes including vascular endothelial growth factor (VEGF), epidermal growth factor (EGF, HB-EGF), fibroblast growth factor (FGF-21), and nerve growth factor inducible (VGF), several of which are known mediators of liver regeneration[8,14,15]. VGF is a 68-kDa precursor polypeptide whose expression in neuronal and neuroendocrine cells is induced by various neurotrophic (NGF, BDGF) and transcription factors [cyclic AMP responsive element-binding protein 1 (CREB)][16,17]. However, few studies have examined the role of VGF expression in cancer cells and its role in the liver, and liver regenerative response is unknown[18–23]. As such, these findings raise the following questions: i) Do heat stress and hepatic thermal ablation induce VGF protein expression and secretion? and ii) If so, is VGF expressed locally within the liver and/or systemically?

The aims of the present study were to test the hypothesis that heat stress and hepatic thermal ablation induce VGF expression and to determine intrahepatic versus systemic VGF expression induced by thermal ablation in vivo and in patients.

MATERIALS AND METHODS

Cell Lines

Clone9, N1S1, Hep3B (ATCC, Manassas, VA), Huh7 (JCRB Cell Bank, Japan), and AS30D (DSMZ, Braunschweig, Germany) cell lines were cultured according to supplier recommendations[24].

Antibodies

Anti-VGF (ab69989) antibody was purchased from Abcam (Cambridge, UK), and anti- -actin antibody (sc-1615) was purchased from Santa Cruz Biotechnology (Dallas, TX, USA). Peroxidase-labeled affinity purified anti-rabbit IgG (074-1506) and anti-goat IgG (14-13-06) antibodies were purchased from KPL (Gaithersburg, MD, USA).

Cellular Heat Stress Protocol

Clone9, N1S1, AS30D, Hep3B, and HuH7 cell lines were suspended in complete media in 1.5-ml microcentrifuge tubes and heat stressed for 10 min at 45°C (moderate heat stress) resulting in incomplete cell killing, 50°C (severe heat stress) resulting in complete cell killing, or 37°C (physiologic) heat stress resulting in no cell killing in an isothermic water bath[24]. Treatment temperature was monitored using an Omega HH41 digital thermometer (Omega Engineering, Stamford, CT, USA) and maintained to within ±0.05°C. Adherent cell lines were prepared following dissociation using nonenzymatic cation-free HBSS/0.5% EDTA. Cells were harvested and either plated in tissue culture plates or rinsed in 1 PBS and snap frozen in liquid N_2 for molecular analyses.

qRT-PCR

Total RNA was extracted with the RNEasy Kit (Qiagen, Valencia, CA, USA), and cDNA was synthesized using the iScript cDNA synthesis Kit (Bio-Rad Laboratories, Inc., Hercules, CA, USA) per the manufacturer's instruction. cDNA was amplified with rat- or human-specific VGF primers [rat VGF: 5 -TGCCGGAC TGGAACGAAGTA-3 (forward), 5 -CCGCGGCCGAA TGTAGTTTG-3 (reverse); human VGF: 5 -CGCCAGA CCTCGACCGT-3 (forward), 5 -GACAGCTGGTGTC ACGACG-3 (reverse)] and SsoAdvanced Universal SYBR Green Supermix on a Bio-Rad CFX96 Real Time Thermocycler System (Bio-Rad). Rat and human 18S were used as housekeeping genes [rat 18S: 5 -TGCCCCTCC TGCCAGAACCA-3 (forward), 5 -GCTGCCTCTGGC TCCCAACG-3 (reverse); human 18S: 5 -CTCAACAC GGGAAACCTCAC-3 (forward), 5 -GCGTCCACCAA CTAAGAACG-3 (reverse)]. Data from each gene were normalized over 18S, and 1- to 10-h heat stressed data were compared to baseline VGF expression within each cell line to calculate fold change from baseline.

Western Blotting

Whole-cell lysates or tissue homogenates were separated by SDS-PAGE, electrophoretically transferred to PVDF, and blotted for VGF (1:500) or beta-actin (1:1,000) per the manufacturer's instruction, and then incubated with corresponding peroxidase-labeled secondary antibodies (1:8,000), incubated with enhanced chemiluminesence (ECL; Pierce, Thermo Fisher, Minneapolis, MN, USA), exposed to film (Kodak/Carestream, Rochester, NY, USA), and developed using a Kodak X-Omat M20 processor[24].

Enzyme-Linked Immunosorbent Assay (ELISA)

Cell culture supernatant and rat and human serum were analyzed for VGF expression using ELISA kits specific for rat or human VGF (LifeSpan BioSciences, Inc., Seattle, WA, USA). VGF concentrations (ng/ml) were compared to 24-h post-heat stress 37°C physiologic control in vitro or baseline (preablation) in vivo and in patients to calculate fold change.

Quantitative Mass Spectrometry (LC-MS/MS) and Phosphoproteomic Pathway Analysis

Per Cell Signaling Technology (CST; Danvers, MA, USA) protocol, samples were analyzed using the PTM Scan method as previously described[25–27]. Briefly, cellular extracts were prepared in urea lysis buffer, sonicated, centrifuged, reduced with DTT, and alkylated with iodoacetamide. Total protein (15 mg) for each sample was digested with trypsin and purified over C18 columns for enrichment with the phosphotyrosine pY-1000 antibody (#8803) and the multipathway reagent or digested with

LysC for the Basophilic Motif Antibody Mix (#32948)[25]. Enriched peptides were purified over C18 STAGE tips[28]. Enriched LysC peptides were subjected to secondary digest with trypsin and second STAGE tip prior to LC-MS/MS analysis.

Replicate injections of each sample were run non-sequentially for each enrichment. Peptides were eluted using a 90- or 120-min linear gradient of acetonitrile in 0.125% formic acid delivered at 280 nl/min. Tandem mass spectra were collected in a data-dependent manner with a QExactive mass spectrometer running XCalibur 2.0.7 SP1 using a top-twenty MS/MS method, a dynamic repeat count of one, and a repeat duration of 30 s. Real-time recalibration of mass error was performed using lock mass with a singly charged polysiloxane ion m/z = 371.101237[29].

MS/MS spectra were evaluated using SEQUEST and the Core platform from Harvard University[30–32]. Files were searched against the NCBI *Rattus norvegicus* FASTA database updated on May 22, 2015. A mass accuracy of ±5 ppm was used for precursor ions and 0.02 Da for product ions. Enzyme specificity was limited to trypsin or LysC/trypsin, with at least one LysC or tryptic (K- or R-containing) terminus required per peptide and up to four miscleavages allowed. Cysteine carboxamidomethylation was specified as a static modification; oxidation of methionine and phosphorylation on serine, threonine, and tyrosine residues were allowed as variable modifications. Reverse decoy databases were included for all searches to estimate false discovery rates and filtered using a 5% FDR in the Linear Discriminant module of Core. Peptides were also manually filtered using a ±5-ppm mass error range and reagent-specific criteria. For each antibody reagent, results were filtered to include only phosphopeptides matching the sequence motif(s) targeted by the antibodies included. All quantitative results were generated using Progenesis V4.1 (Waters Corporation) to extract the integrated peak area of the corresponding peptide assignments. Accuracy of quantitative data was ensured by manual review in Progenesis or in the ion chromatogram files.

The protein interaction networks were generated from the Ingenuity Pathway Analysis (IPA; Qiagen Inc., https://www.qiagenbioinformatics.com/products/ingenuity-pathway-analysis) as previously described[26,33]. Core analyses were run on the entire combined dataset as well as on a subset of the data that showed changes in abundance with treatment. Only direct interactions were used, with experimental and high confidence predicted interactions allowed. Protein nodes were color coded by the fold changes for all the peptides identified from that protein to indicate peptides that increased (green), decreased (red), did not change (gray), or both increased/decreased (yellow) with the indicated treatment.

Hepatic Thermal Ablation in an Orthotopic N1S1 HCC Model

All animal studies were approved by the Institutional Animal Care and Use Committee. The N1S1 orthotopic HCC model was developed in male Sprague–Dawley rats (400–500 g; Harlan/Envigo Laboratories, Indianapolis, IN, USA)[34]. Immediately following N1S1 cell injection (3 10^6 cells) into the median hepatic lobe, rats were randomized to hepatic laser ablation in the HCC cell-bearing median hepatic lobe with an energy dose of 3 W for 90 s or sham ablation using an FDA-approved 980-nm laser generator (Visualase, Houston, TX, USA) (n 6 per experimental group)[34–36]. The laser fiber was inserted but not activated for sham-ablated animals.

Animals were euthanized on days 0, 1, 3, and 7 post-ablation (n = 6 per time point and ablation treatment). Normal and ablated liver and tumor were sectioned and formalin fixed and paraffin embedded (FFPE) for immunohistochemical analysis, or snap frozen in liquid N_2 for immunoblot analysis from tissue homogenates. Blood was allowed to clot before centrifugation at 2,000 rpm for 10 min at 4°C. The serum was then extracted and stored at −80°C.

Gross and Microscopic Pathology

Liver/tumor tissue was removed and cut into 2-mm cross sections encompassing the ablation zone. All specimens were FFPE. FFPE sections were stained with hematoxylin–eosin (H&E) or antibodies against VGF (1:200) per the manufacturer's instruction as previously described[24]. All sections were reviewed in a blinded and random fashion.

Clinical HCC Ablation Study

This study was approved by the Institutional Review Board (IRB 13-000922). Patients undergoing clinically indicated thermal ablation for HCC were considered for this study. Written and verbal informed consents were obtained from all study participants, and the signed consent form was scanned into each patient's electronic medical record. Peripheral blood (10 ml) was collected at three time points: 1) preablation baseline, 2) 3–6 h post-ablation, and 3) 18–24 h postablation. These time points were selected based on previous studies examining the kinetics of the priming and progression phase of the liver regenerative response triggered by liver injury, which demonstrated significant increases in growth factor and cytokine expression within the first 24 h. A standardized blood collection and processing protocol was utilized. A nurse from the clinical research unit performed peripheral venipuncture to obtain whole blood in a red top tube. Samples were allowed to clot at room temperature for a minimum of 30 min, centrifuged at 3,000 revolutions per minute (RPM) for 15 min at 4°C, and then the serum was

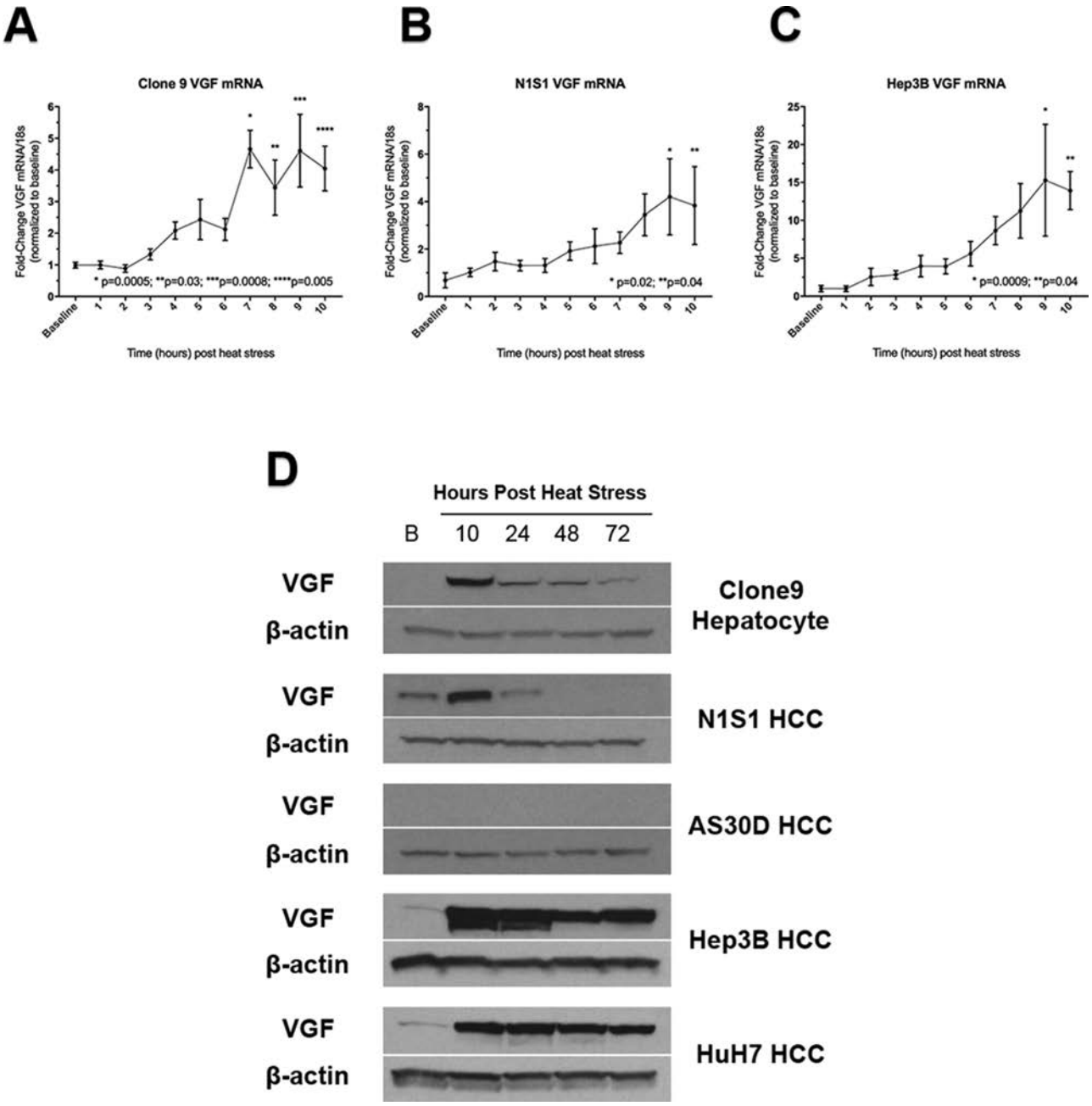

Figure 1. Moderate heat stress induces nerve growth factor inducible (VGF) mRNA and protein expression in hepatocytes and hepatocellular carcinoma (HCC) cells in vitro. (A–C) Fold change relative to baseline in VGF mRNA expression in (A) clone 9 hepatocyte, (B) N1S1 HCC, and (C) Hep3B HCC cell lines at 0–10 h following moderate heat stress (45°C 10 min). Data are presented as mean±SEM of four independent experiments and were analyzed using one-way analysis of variance (ANOVA) followed by post hoc pairwise comparison using Dunnett's test compared to baseline (control group). (D) Western blotting of VGF protein expression in hepatocytes and HCC cell lines at baseline (B) and 10–72 h following moderate heat stress (45°C 10 min). -Actin was used as a loading control. Representative blots from one of four independent experiments.

aliquoted into 1.5-ml microcentrifuge tubes and frozen at −80°C.

Demographic, clinical, imaging, ablation procedure, and follow-up data were collected from the electronic medical record.

Statistical Analysis

Statistical analyses were performed using Prism 7.0 (GraphPad Software, Inc., La Jolla, CA, USA). Differences between groups were compared using ordinary or repeated-measures one-way analysis of variance (ANOVA)

followed by post hoc pairwise comparison with Dunnett's test. For *t*-tests, since sample sizes for comparisons were similar, if standard deviations were not more than double another standard deviation within the same group, equal variance was assumed, otherwise unequal variance was assumed.[37] Two-sided $p < 0.05$ was considered statistically significant.

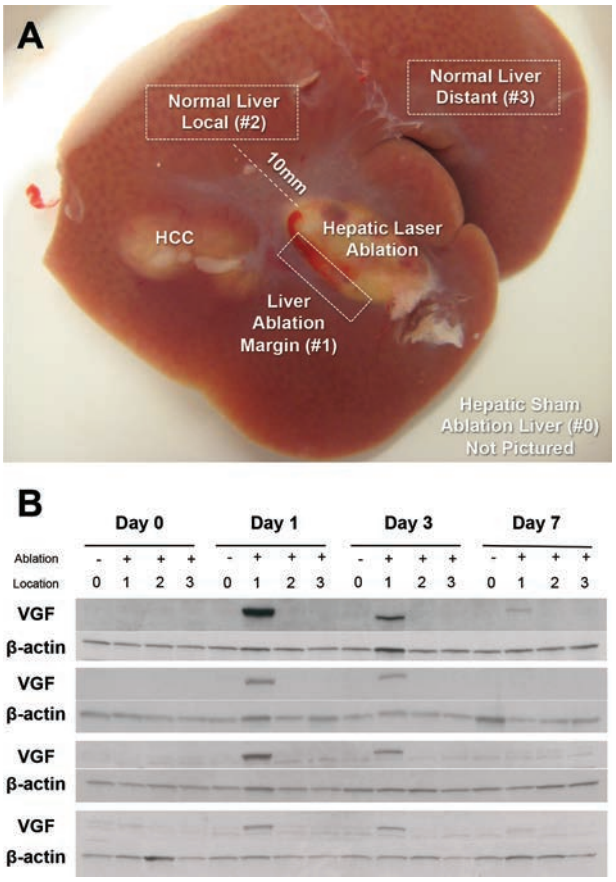

Figure 2. Hepatic thermal ablation induces local intrahepatic VGF expression at the ablation margin but not in the distant intrahepatic lobe or sham ablated liver in vivo. (A) Representative gross pathologic photograph of the hepatic ablation zone shows the anatomic locations in the liver where tissue was harvested for Western blotting. #0 = Normal liver adjacent to the laser fiber in the sham ablation group (not pictured); #1 = normal, non-ablated liver in the median hepatic lobe approximately 10 mm from the ablation zone; #2 = the hepatic ablation margin including both ablated and non-ablated livers; #3 = normal, non-ablated liver in the distant intrahepatic liver in the left hepatic lobe. (B) Representative Western blots from tissue harvested from laser and sham ablation groups at 0–7 days postablation ($n = 4$ independent animals—biological replicates—per Western blot) show a time-dependent increase in VGF expression at the ablation margin (#2) beginning 1 day postablation and decreasing from 3 to 7 days postablation. There is no VGF expression in normal liver remote from the ablation zone (#1) or in normal liver in the distant liver (#3) or in the sham ablation group (#0). -Actin was used as a loading control.

RESULTS

Moderate Heat Stress Induces VGF Expression and Secretion in Hepatocytes and HCC Cells

Moderate heat stress induced a time-dependent increase in VGF mRNA expression compared to baseline in hepatocytes (3.4- to 7.4-fold; $p = 0.03$) (Fig. 1A) and HCC cells (3.8- to 15.3-fold; $p = 0.04$) (Fig. 1B and C) at 7–10 h post-heat stress. Similarly, moderate heat stress induced a time-dependent increase in VGF protein expression compared to baseline in hepatocytes and HCC cells beginning at 10 h post-heat stress and decreasing over the next 72 h (Fig. 1D). Additionally, moderate heat stress induced increased VGF protein secretion into the supernatant compared to the 37°C control group at 24–48 h post-heat stress in the N1S1 HCC cell line (3.1-fold; $p < 0.05$) and at 72 h in the Hep3B HCC cell line (3.3-fold; $p < 0.05$).

Hepatic Thermal Ablation Induces Local Intrahepatic VGF Expression In Vivo

Hepatic thermal ablation induced increased VGF protein expression at the hepatic ablation margin beginning at 1 day postablation and decreasing by 3 and 7 days postablation (Figs. 2 and 3). However, there was no increased VGF protein expression in normal liver remote from the ablation zone or in the distant

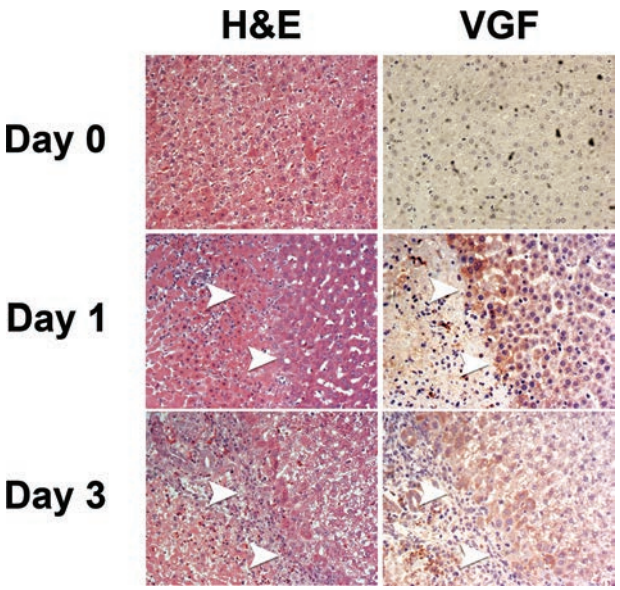

Figure 3. Hepatic thermal ablation induces VGF expression at the hepatic ablation margin. Representative photomicrographs (magnification; 20) from hematoxylin and eosin- (H&E; left column) and VGF-immunostained sections (right column) at 0–3 days postablation show VGF immunostaining at the hepatic ablation margin beginning at 1 day postablation (white arrowheads).

Table 1. Demographic, Clinical, Ablation, VGF Expression, and Follow-up Data for 16 Patients Undergoing Image-Guided Percutaneous Radiofrequency (RFA) or Microwave (MWA) Ablation for Hepatocellular Carcinoma (HCC)

Age/ Gender	Liver Disease	Cirrhotic Morphology	Prior Treatment	No. of HCC	Size (cm)	Ablation Device	Probes × Time	VGF 3–6 h Versus Baseline	VGF 18–24 h Versus Baseline	Follow-up (Months)	Local Recurrence	New Intrahepatic Disease	Status	Notes
70/M	NASH	Yes	None	1	2.0	RFA	2 12.5	0.85	0.84	22.3	No	Yes	Dead	–
60/M	NASH	Yes	TACE	1	1.2	MWA	2 10	0.79	0.88	42.3	No	Yes	Alive	Subsequent transplant; NED
65/M	EtOH	Yes	None	1	3.7	MWA	2 10	0	0	35.9	No	No	Alive	
67/F	None	No	Resection	1	1.2	RFA	2 7	1.5	0.98	23.4	Yes	Yes	Alive	
73/F	EtOH	Yes	RFA	1	1.9	RFA	2 13	0	0	17.0	Yes	No	Dead	
71/F	NASH	Yes	RFA	1	1.6	RFA	3 8	0.83	0.86	27.2	No	No	Dead	
62/M	HCV, EtOH, NASH	Yes	None	1	2.1	RFA	2 8	0.71	0.75	38.4	No	No	Alive	
60/M	EtOH	Yes	None	1	2.3	MWA	2 5	1.1	1.0	36.8	No	Yes	Alive	Subsequent transplant; NED
61/M	EtOH	Yes	None	1	2.5	MWA	2 15	1.1	0.96	31.4	No	No	Alive	
67/F	NASH	Yes	None	1	1.5	RFA	2 10	0.81	0.88	34.1	No	No	Alive	
71/M	NASH	Yes	RFA	1	1.8	MWA	2 8	0.85	0.80	16.0	No	No	Alive	
55/F	HCV	Yes	TACE	3	1.6	MWA	1 5	1.1	1.0	32.5	No	Yes	Alive	Subsequent transplant, developed recurrent HCC in allograft and bone metastases
					4.5		3 10							
					1.5		1 5							
57/M	HCV	Yes	None	2	1.6	MWA	1 6	0.90	0.81	32.2	No	No	Alive	Subsequent transplant; NED
					1.2		1 7							
58/M	HCV	Yes	None	2	2.3	MWA	2 10	0.78	0.63	7.1	Yes	No	Alive	Repeat RFA of recurrence
					2.6		2 5							
76/M	EtOH	Yes	None	1	3.3	MWA	2 10	0.88	0.84	26.0	Yes	Yes	Alive	Subsequent TACE
82/M	EtOH	Yes	None	1	3.4	RFA	3 10	0.79	0.73	8.8	No	No	Dead	

VGF, nerve growth factor inducible; NASH, non-alcoholic steatohepatitis; EtOH, alcoholic liver disease; HCV, hepatitis C virus; TACE, transarterial chemoembolization; NED, no evidence of disease. VGF data reported as fold change from baseline.

intrahepatic lobe in the thermal ablation group or in the liver in the sham ablation group at any time point (Fig. 2). Immunohistochemistry showed increased VGF staining at the thermal ablation margin beginning at 24 h post-ablation with decreasing VGF staining as distance from the ablation zone increased (Fig. 3).

Thermal Ablation Does Not Induce Increased Expression of VGF in Serum in a Preclinical HCC Model or in Patients Undergoing Radiofrequency or Microwave Ablation for HCC

There was no detectable serum VGF (0 ng/ml) in rats in the hepatic ablation or sham ablation groups at any time point postablation.

Demographic, clinical, ablation, serum VGF, and follow-up data for 16 patients undergoing radiofrequency or microwave ablation are summarized in Table 1. There was no significant change in serum VGF following HCC thermal ablation in patients at 3–6 and 18–24 h postablation compared to baseline (0.71- and 0.63-fold; $p = 0.27$ and $p = 0.16$, respectively). At an average follow-up of 27.0 months (range: 7.1 to 42.3 months), four patients (25%) developed local HCC tumor recurrence, six patients (37.5%) developed new intrahepatic HCC, and four patients (25%) died. Additionally, four patients (25%) underwent orthotopic liver transplantation, with no evidence of disease in three and allograft recurrence in one.

Moderate Heat Stress Induces CREB1 Transcription Factor Activation

IPA of quantitative mass spectrometry data showed that moderate heat stress induced nerve growth factor (NGF) signaling, AKT and ERK proteins, and CREB1 transcription factor activation (z-score = 2.5, $p = 0.005$), a known transcription factor for VGF (Fig. 4).

DISCUSSION

Our data show that moderate (45°C) heat stress of HCC cells and hepatocytes induces rapid transcription, translation, and secretion of VGF in vitro and a time-

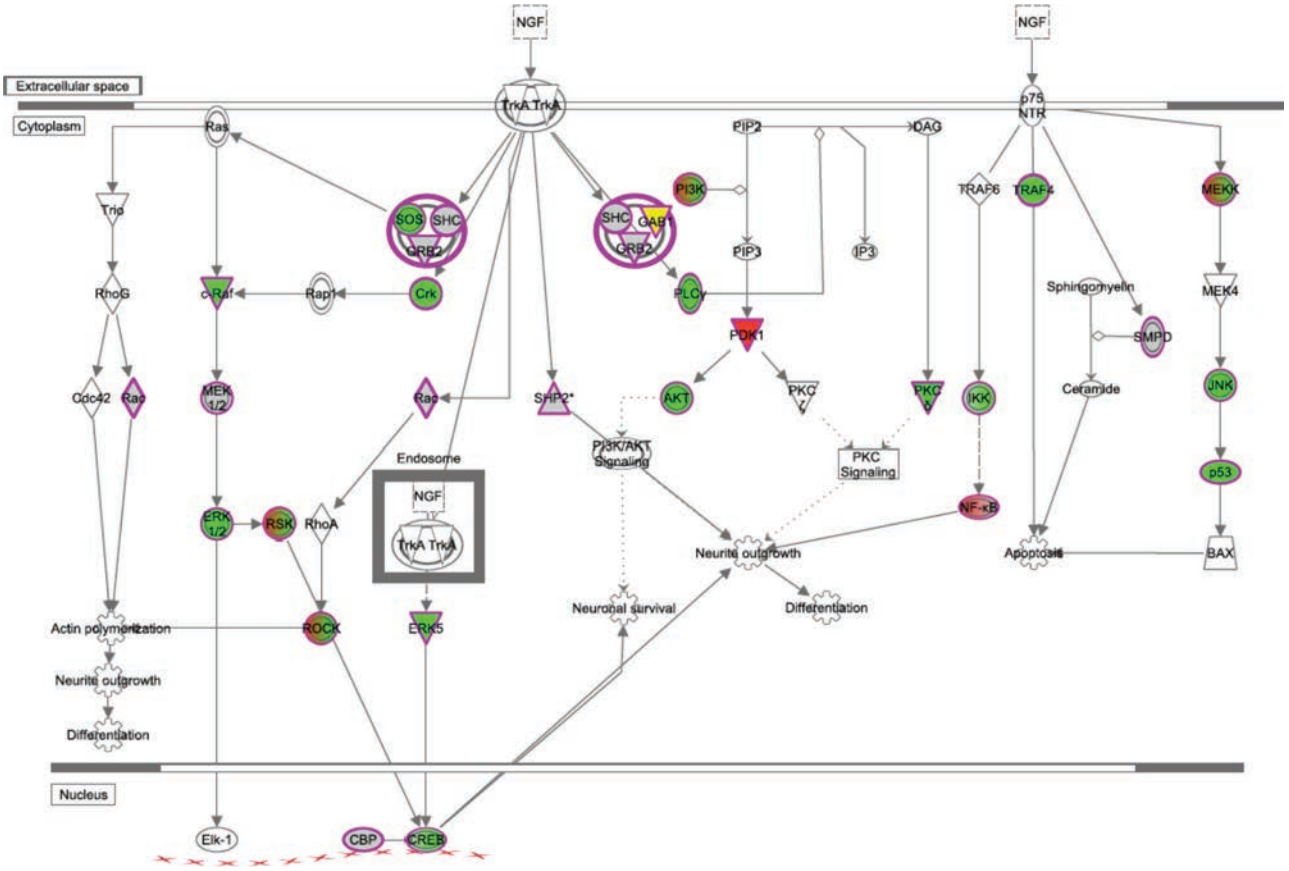

Figure 4. Moderate heat stress induces nerve growth factor (NGF) signaling including downstream activation of AKT and ERK as well as cyclic AMP responsive element-binding protein 1 (CREB1) transactivation. The protein interaction network was generated from the Ingenuity Pathway Analysis (IPA; Qiagen Inc., https://www.qiagenbioinformatics.com/products/ingenuity-pathway-analysis). IPA of quantitative phosphoproteomic data identifies activation of numerous NGF pathway signaling proteins (green, increased phosphorylation; red, decreased phosphorylation; gray, neutral; yellow, both increases and decreases).

dependent increase in VGF expression at the liver ablation margin in vivo, but not in the distant hepatic lobe or serum. Moreover, proteomic and bioinformatics analyses identified NGF/ERK signaling and CREB1 transcription factor activation as candidate mechanisms mediating heat stress-induced VGF expression. Taken together, these findings suggest that thermal ablation-induced VGF expression may be mediated by ERK/CREB1 signaling and localized within the liver near the ablation zone.

VGF expression can be induced by a number of neurotrophins including NGF. Of note, it has been reported that the VGF gene contains a putative silencer element in the promoter region, which prevents expression in nonneuronal cells.[38] However, our findings suggest that hepatocytes and HCC cells express VGF under basal conditions, and VGF expression is further induced by moderate heat stress in vitro and hepatic thermal ablation in vivo. Moreover, following protein translation, the VGF polypeptide precursor undergoes posttranslational cleavage into multiple biologically active neuroendocrine secretory peptides including TLQP-21 and AQEE-30, which have been shown to play a role in the regulation of energy balance and metabolism, synaptic strengthening, and antidepressant activity[16,17,39,40]. These VGF neuroendocrine secretory peptides have been shown to participate in intercellular communication and signal via the PI3K/mTOR/AKT and mitogen-activated protein kinase (MAPK) pathways[16,17,41–43]. Prior studies have identified both moderate heat stress and thermal ablation-induced ERK signaling at the ablation margin in two biologically distinct HCC models and PI3K/mTOR/AKT signaling as a candidate mediator of thermal ablation-induced HCC growth in vivo[8,24]. However, few studies have examined the role of VGF in cancer cells including breast, lung, and neuroendocrine cancers but not HCC, and its roles in the liver and liver regenerative response are unknown[18–23,44]. Although speculative, the findings of early upregulation and secretion of VGF within the first 10–24 h following heat stress and hepatic thermal ablation and subsequent decrease over the next 3–7 days postablation coincide with the initiation, proliferation, and termination phases of liver regeneration[15]. Taken together, our findings not only suggest a potential neurotrophin-independent mechanism of heat stress and thermal ablation-induced VGF expression in nonneuroendocrine cells but also provide a rationale for further studies investigating a potential role of VGF in liver regeneration and HCC tumorigenesis.

Of note, there was no increased VGF in the serum following thermal ablation despite increased VGF expression near the hepatic ablation zone. Prior preclinical and clinical studies examining hepatectomy or thermal ablation-induced growth factor expression have yielded conflicting results regarding growth factor expression, which may in part be related to time course and tissue or blood compartment measured[45–52]. Consequently, changes in thermal ablation-induced growth factors in the liver near the ablation zone may not be reflected systemically in the serum, which may limit the use of serum growth factor levels as biomarkers and require targeted evaluation of tissue near the ablation margin. Nonetheless, given that the VGF polypeptide precursor undergoes posttranslational cleavage into biologically active neuroendocrine secretory peptides including TLQP-21 and AQEE-30, it is possible that the VGF ELISA assays used in these studies do not have cross-reactivity for these VGF cleavage products, thereby potentially resulting in false-negative findings in the serum. As such, further studies are needed to specifically assay for these VGF cleavage peptides using peptide-specific ELISA assays or advanced proteomics techniques such as quantitative mass spectrometry[13].

Recent studies have identified several biological mechanisms as candidate mediators of thermal ablation-induced HCC growth including inflammatory signaling—IL-6, COX-2, and STAT-3 signaling—hepatocyte growth factor signaling (HGF/cMET), epidermal growth factor signaling (EGF/EGFR), and PI3K/mTOR/AKT signaling[7–13]. Additionally, Jondal et al. identified numerous growth factor families whose expression is induced by moderate heat stress in both HCC cells and hepatocytes including vascular endothelial (VEGF), epidermal (EGF, HB-EGF), fibroblast (FGF-21), insulin-like (IGF-2), and transforming (TGF- and -) growth factor[8]. As such, heat stress and hepatic thermal ablation may fundamentally induce a liver regenerative response mediated by a complex interplay between inflammatory and growth factors, thereby stimulating local liver regeneration and growth of any residual HCC cells within the vicinity of the ablation zone. Clinically, aggressive HCC recurrence following thermal ablation has been reported intrasegmentally, which supports local intrahepatic growth mechanisms as mediating thermal ablation-induced HCC growth[6].

There are limitations to these studies. These present experiments identified VGF as a growth factor induced by moderate heat stress and hepatic thermal ablation but do not establish mechanistically VGF as a mediator or liver regeneration or thermal ablation-induced HCC tumorigenesis. Further studies are needed to determine not only the regulation of heat stress and thermal ablation-induced VGF expression in hepatocytes and HCC cells but also the functional role of VGF in liver regeneration and thermal ablation-induced tumorigenesis. One of the key challenges is that, currently, there are no small molecule inhibitors or neutralizing antibodies for inhibiting VGF. As such, development of genetic models utilizing VGF gain- and loss-of-function techniques will be critical tools for further studies on the biological role of VGF. Additionally, the in vivo experiments were limited to one orthotopic HCC model utilizing laser ablation. However,

further studies are needed in additional preclinical HCC models utilizing different ablation devices in order to better understand the generalizability of these findings[53–56]. Next, heat stress induced VGF mRNA but not protein expression in the AS30D HCC cell line, thereby highlighting a potential limitation and pitfall of trying to extrapolate biological information from gene expression alone rather than protein expression and function. As such, further studies are needed to better understand the posttranscriptional regulation of VGF protein translation in different HCC cell lines. Furthermore, only serum VGF levels were measured in patients. However, given the findings of thermal ablation-induced local intrahepatic VGF expression in a rat HCC model, further studies need to validate these findings in patients with biopsy of the ablation margin at 24–72 h postablation. Furthermore, prior gene expression screening studies identified several growth factors induced by heat stress beyond VGF, including VEGF-A, FGF-21, and HB-EGF, which warrant further investigation. Last, further studies are needed to validate CREB1 transactivation as a mediator of heat stress-induced VGF expression with both biochemical methods and functional assays in both in vitro and in vivo models.

In conclusion, moderate heat stress and hepatic thermal ablation induce local but not distant intrahepatic or systemic VGF expression and may in part be mediated by CREB1 transcription factor activation. These experiments identify a potential noncanonical neurotrophin-independent mechanism of heat stress and hepatic thermal ablation-induced VGF expression in nonneuroendocrine cells. Last, VGF warrants further investigation as a potential growth factor involved in the liver response to injury and regeneration as well as HCC tumorigenesis.

ACKNOWLEDGMENTS: Research support provided in part by the Society of Interventional Radiology (SIR) Foundation (http://www.sirfoundation.org/) Allied Scientist Training Grant, Mayo Clinic Center for Clinical and Translational Science (CCaTS; http://www.mayo.edu/ctsa) through Grant No. UL1 RR024150 from the National Center for Research Resources (NCRR), a component of the NIH and NIH Grant No. R01 CA177686 from the National Cancer Institute (NCI). The funding sources did not play any role in the study design, data collection or analysis, decision to publish, or preparation of the manuscript. Dr. Thompson's M.D., Ph.D. training was supported by Mayo Clinic Center for Clinical and Translational Science (CCaTS) M.D./Ph.D. in Clinical and Translational Science TL1 RR024152 and TL1 TR000137. The contents herein are solely the responsibility of the authors and do not necessarily represent the official views of the NIH. The authors declare no conflicts of interest.

REFERENCES

1. Chinnaratha MA, Chuang MY, Fraser RJ, Woodman RJ, Wigg AJ. Percutaneous thermal ablation for primary hepatocellular carcinoma: A systematic review and meta-analysis. J Gastroenterol Hepatol. 2016;31(2):294–301.
2. Ruzzenente A, Manzoni GD, Molfetta M, Pachera S, Genco B, Donataccio M, Guglielmi A. Rapid progression of hepatocellular carcinoma after radiofrequency ablation. World J Gastroenterol. 2004;10(8):1137–40.
3. Angonese C, Baldan A, Cillo U, D'Alessandro A, De Antoni M, De Giorgio M, Masotto A, Marino D, Massani M, Mazzucco M and others. Complications of radiofrequency thermal ablation in hepatocellular carcinoma: What about "explosive" spread? Gut 2006;55(3):435–6.
4. Shiozawa K, Watanabe M, Takahashi M, Wakui N, Iida K, Sumino Y. Analysis of patients with rapid aggressive tumor progression of hepatocellular carcinoma after percutaneous radiofrequency ablation. Hepatogastroenterology 2009;56(96):1689–95.
5. Kei SK, Rhim H, Choi D, Lee WJ, Lim HK, Kim YS. Local tumor progression after radiofrequency ablation of liver tumors: Analysis of morphologic pattern and site of recurrence. AJR Am J Roentgenol. 2008;190(6):1544–51.
6. Kang TW, Lim HK, Lee MW, Kim YS, Rhim H, Lee WJ, Gwak GY, Paik YH, Lim HY, Kim MJ. Aggressive intrasegmental recurrence of hepatocellular carcinoma after radiofrequency ablation: Risk factors and clinical significance. Radiology 2015;276(1):274–85.
7. Rozenblum N, Zeira E, Scaiewicz V, Bulvik B, Gourevitch S, Yotvat H, Galun E, Goldberg SN. Oncogenesis: An "off-target" effect of radiofrequency ablation. Radiology 2015;276(2):426–32.
8. Jondal DE, Thompson SM, Butters KA, Knudsen BE, Anderson JL, Carter RE, Roberts LR, Callstrom MR, Woodrum DA. Heat stress and hepatic laser thermal ablation induce hepatocellular carcinoma growth: Role of PI3K/mTOR/AKT signaling. Radiology 2018;299(3):730–8.
9. Kumar G, Goldberg SN, Gourevitch S, Levchenko T, Torchilin V, Galun E, Ahmed M. Targeting STAT3 to suppress systemic pro-oncogenic effects from hepatic radiofrequency ablation. Radiology 2017;286(2):524–36.
10. Kumar G, Goldberg SN, Wang Y, Velez E, Gourevitch S, Galun E, Ahmed M. Hepatic radiofrequency ablation: Markedly reduced systemic effects by modulating periablational inflammation via cyclooxygenase-2 inhibition. Eur Radiol. 2017;27(3):1238–47.
11. Ahmed M, Kumar G, Moussa M, Wang Y, Rozenblum N, Galun E, Goldberg SN. Hepatic radiofrequency ablation-induced stimulation of distant tumor growth is suppressed by c-Met inhibition. Radiology 2016;279(1):103–17.
12. Rozenblum N, Zeira E, Bulvik B, Gourevitch S, Yotvat H, Galun E, Goldberg SN. Radiofrequency ablation: Inflammatory changes in the periablative zone can induce global organ effects, including liver regeneration. Radiology 2015; 276(2):416–25.
13. Thompson SM, Jondal DE, Butters KA, Knudsen BE, Anderson JL, Stokes MP, Jia X, Grande JP, Roberts LR, Callstrom MR, and others. Heat stress induced, ligand-independent MET and EGFR signalling in hepatocellular carcinoma. Int J Hyperthermia 2017;34(6):812–23.
14. Bohm F, Kohler UA, Speicher T, Werner S. Regulation of liver regeneration by growth factors and cytokines. EMBO Mol Med. 2010;2(8):294–305.
15. Jia C. Advances in the regulation of liver regeneration. Expert Rev Gastroenterol Hepatol. 2011;5(1):105–21.
16. Ferri GL, Noli B, Brancia C, D'Amato F, Cocco C. VGF: An inducible gene product, precursor of a diverse array of neuro-endocrine peptides and tissue-specific disease biomarkers. J Chem Neuroanat. 2011;42(4):249–61.

17. Lewis JE, Brameld JM, Jethwa PH. Neuroendocrine role for VGF. Front Endocrinol. (Lausanne) 2015;6:3.
18. Hwang W, Chiu YF, Kuo MH, Lee KL, Lee AC, Yu CC, Chang JL, Huang WC, Hsiao SH, Lin SE, and others. Expression of neuroendocrine factor VGF in lung cancer cells confers resistance to EGFR kinase inhibitors and triggers epithelial-to-mesenchymal transition. Cancer Res. 2017;77(11):3013–26.
19. Matsumoto T, Kawashima Y, Nagashio R, Kageyama T, Kodera Y, Jiang SX, Okayasu I, Kameya T, Sato Y. A new possible lung cancer marker: VGF detection from the conditioned medium of pulmonary large cell neuroendocrine carcinoma-derived cells using secretome analysis. Int J Biol Markers 2009;24(4):282–5.
20. Annaratone L, Medico E, Rangel N, Castellano I, Marchio C, Sapino A, Bussolati G. Search for neuro-endocrine markers (chromogranin A, synaptophysin and VGF) in breast cancers. An integrated approach using immunohistochemistry and gene expression profiling. Endocr Pathol. 2014;25(3):219–28.
21. Rindi G, Licini L, Necchi V, Bottarelli L, Campanini N, Azzoni C, Favret M, Giordano G, D'Amato F, Brancia C, and others. Peptide products of the neurotrophin-inducible gene vgf are produced in human neuroendocrine cells from early development and increase in hyperplasia and neoplasia. J Clin Endocrinol Metab. 2007;92(7):2811–5.
22. Akhter S, Chakraborty S, Moutinho D, Alvarez-Coiradas E, Rosa I, Vinuela J, Dominguez E, Garcia A, Requena JR. The human VGF-derived bioactive peptide TLQP-21 binds heat shock 71 kDa protein 8 (HSPA8)on the surface of SH-SY5Y cells. PLoS One 2017;12(9):e0185176.
23. Brait M, Maldonado L, Noordhuis MG, Begum S, Loyo M, Poeta ML, Barbosa A, Fazio VM, Angioli R, Rabitti C, and others. Association of promoter methylation of VGF and PGP9.5 with ovarian cancer progression. PLoS One 2013;8(9):e70878.
24. Thompson SM, Callstrom MR, Jondal DE, Butters KA, Knudsen BE, Anderson JL, Lien KR, Sutor SL, Lee JS, Thorgeirsson SS, and others. Heat stress-induced PI3K/mTORC2-dependent AKT signaling is a central mediator of hepatocellular carcinoma survival to thermal ablation induced heat stress. PLoS One 2016;11(9):e0162634.
25. Stokes MP, Farnsworth CL, Moritz A, Silva JC, Jia X, Lee KA, Guo A, Polakiewicz RD, Comb MJ. PTMScan direct: Identification and quantification of peptides from critical signaling proteins by immunoaffinity enrichment coupled with LC-MS/MS. Mol Cell Proteomics 2012; 11(5):187–201.
26. Stokes MP, Farnsworth CL, Gu H, Jia X, Worsfold CR, Yang V, Ren JK, Lee KA, Silva JC. Complementary PTM profiling of drug response in human gastric carcinoma by immunoaffinity and IMAC methods with total proteome analysis. Proteomes 2015;3(3):160–83.
27. Rush J, Moritz A, Lee KA, Guo A, Goss VL, Spek EJ, Zhang H, Zha XM, Polakiewicz RD, Comb MJ. Immunoaffinity profiling of tyrosine phosphorylation in cancer cells. Nature Biotechnol. 2005;23(1):94–101.
28. Rappsilber J, Ishihama Y, Mann M. Stop and go extraction tips for matrix-assisted laser desorption/ionization, nanoelectrospray, and LC/MS sample pretreatment in proteomics. Anal Chem. 2003;75(3):663–70.
29. Olsen JV, de Godoy LM, Li G, Macek B, Mortensen P, Pesch R, Makarov A, Lange O, Horning S, Mann M. Parts per million mass accuracy on an Orbitrap mass spectrometer via lock mass injection into a C-trap. Mol Cell Proteomics 2005;4(12):2010–21.
30. Villen J, Beausoleil SA, Gerber SA, Gygi SP. Large-scale phosphorylation analysis of mouse liver. Proc Natl Acad Sci USA 2007;104(5):1488–93.
31. Huttlin EL, Jedrychowski MP, Elias JE, Goswami T, Rad R, Beausoleil SA, Villen J, Haas W, Sowa ME, Gygi SP. A tissue-specific atlas of mouse protein phosphorylation and expression. Cell 2010;143(7):1174–89.
32. Eng JK, McCormack AL, Yates JR. An approach to correlate tandem mass spectral data of peptides with amino acid sequences in a protein database. J Am Soc Mass Spectrom. 1994;5(11):976–89.
33. Kramer A, Green J, Pollard J Jr, Tugendreich S. Causal analysis approaches in ingenuity pathway analysis. Bioinformatics 2014;30(4):523–30.
34. Thompson SM, Callstrom MR, Knudsen B, Anderson JL, Carter RE, Grande JP, Roberts LR, Woodrum DA. Development and preliminary testing of a translational model of hepatocellular carcinoma for MR imaging and interventional oncologic investigations. J Vasc Interv Radiol. 2012;23(3):385–95.
35. Thompson SM, Callstrom MR, Butters KA, Knudsen B, Grande JP, Roberts LR, Woodrum DA. Heat stress induced cell death mechanisms in hepatocytes and hepatocellular carcinoma: In vitro and in vivo study. Lasers Surg Med. 2014;46(4):290–301.
36. Thompson SM, Callstrom MR, Knudsen BE, Anderson JL, Sutor SL, Butters KA, Kuo C, Grande JP, Roberts LR, Woodrum DA. Molecular bioluminescence imaging as a noninvasive tool for monitoring tumor growth and therapeutic response to MRI-guided laser ablation in a rat model of hepatocellular carcinoma. Invest Radiol. 2013; 48(6):413–21.
37. Campbell MJ, Swinscow TDV. Statistics at square one. Chichester (UK)/Hoboken (NJ): Wiley-Blackwell/BMJ Books; 2009.
38. Possenti R, Di Rocco G, Nasi S, Levi A. Regulatory elements in the promoter region of vgf, a nerve growth factor-inducible gene. Proc Natl Acad Sci USA 1992;89(9):3815–9.
39. Watson E, Fargali S, Okamoto H, Sadahiro M, Gordon RE, Chakraborty T, Sleeman MW, Salton SR. Analysis of knockout mice suggests a role for VGF in the control of fat storage and energy expenditure. BMC Physiol. 2009;9:19.
40. Mizoguchi T, Minakuchi H, Ishisaka M, Tsuruma K, Shimazawa M, Hara H. Behavioral abnormalities with disruption of brain structure in mice overexpressing VGF. Sci Rep. 2017;7(1):4691.
41. Lu Y, Wang C, Xue Z, Li C, Zhang J, Zhao X, Liu A, Wang Q, Zhou W. PI3K/AKT/mTOR signaling-mediated neuropeptide VGF in the hippocampus of mice is involved in the rapid onset antidepressant-like effects of GLYX-13. Int J Neuropsychopharmacol. 2014;18(5).
42. Severini C, Ciotti MT, Biondini L, Quaresima S, Rinaldi AM, Levi A, Frank C, Possenti R. TLQP-21, a neuroendocrine VGF-derived peptide, prevents cerebellar granule cells death induced by serum and potassium deprivation. J Neurochem. 2008;104(2):534–44.
43. Rodriguez-Seoane C, Ramos A, Korth C, Requena JR. DISC1 regulates expression of the neurotrophin VGF through the PI3K/AKT/CREB pathway. J Neurochem. 2015; 135(3):598–605.

44. Jensen K, Marzioni M, Munshi K, Afroze S, Alpini G, Glaser S. Autocrine regulation of biliary pathology by activated cholangiocytes. Am J Physiol Gastrointest Liver Physiol. 2012;302(5):G473–83.
45. Ke S, Ding XM, Kong J, Gao J, Wang SH, Cheng Y, Sun WB. Low temperature of radiofrequency ablation at the target sites can facilitate rapid progression of residual hepatic VX2 carcinoma. J Transl Med. 2010;8:73.
46. Kong J, Kong L, Kong J, Ke S, Gao J, Ding X, Zheng L, Sun H, Sun W. After insufficient radiofrequency ablation, tumor-associated endothelial cells exhibit enhanced angiogenesis and promote invasiveness of residual hepatocellular carcinoma. J Transl Med. 2012;10:230.
47. Meredith K, Haemmerich D, Qi C, Mahvi D. Hepatic resection but not radiofrequency ablation results in tumor growth and increased growth factor expression. Ann Surg. 2007;245(5):771–6.
48. Ohno T, Kawano K, Yokoyama H, Tahara K, Sasaki A, Aramaki M, Kitano S. Microwave coagulation therapy accelerates growth of cancer in rat liver. J Hepatol. 2002; 36(6):774–9.
49. Nijkamp MW, van der Bilt JD, de Bruijn MT, Molenaar IQ, Voest EE, van Diest PJ, Kranenburg O, Borel Rinkes IH. Accelerated perinecrotic outgrowth of colorectal liver metastases following radiofrequency ablation is a hypoxia-driven phenomenon. Ann Surg. 2009;249(5):814–23.
50. Fifis T, Malcontenti-Wilson C, Amijoyo J, Anggono B, Muralidharan V, Nikfarjam M, Christophi C. Changes in growth factor levels after thermal ablation in a murine model of colorectal liver metastases. HPB (Oxford) 2011; 13(4):246–55.
51. Mertens JC, Martin IV, Schmitt J, Frei P, Bruners P, Herweg C, Mahnken AH, Mullhaupt B, Geier A. Multikinase inhibitor sorafenib transiently promotes necrosis after radiofrequency ablation in rat liver but activates growth signals. Eur J Radiol. 2012;81(7):1601–6.
52. Evrard S, Menetrier-Caux C, Biota C, Neaud V, Mathoulin-Pelissier S, Blay JY, Rosenbaum J. Cytokines pattern after surgical radiofrequency ablation of liver colorectal metastases. Gastroenterol Clin Biol. 2007;31(2):141–5.
53. Thompson SM, Callstrom MR, Knudsen B, Anderson JL, Butters KA, Grande JP, Roberts LR, Woodrum DA. AS30D model of hepatocellular carcinoma: Tumorigenicity and preliminary characterization by imaging, histopathology, and immunohistochemistry. Cardiovasc Intervent Radiol. 2013;36(1):198–203.
54. Cho HR, Choi JW, Kim HC, Song YS, Kim GM, Son KR, Chung JW. Sprague-Dawley rats bearing McA-RH7777 cells for study of hepatoma and transarterial chemoembolization. Anticancer Res. 2013;33(1):223–30.
55. Katzenellenbogen M, Mizrahi L, Pappo O, Klopstock N, Olam D, Jacob-Hirsch J, Amariglio N, Rechavi G, Domany E, Galun E and others. Molecular mechanisms of liver carcinogenesis in the mdr2-knockout mice. Mol Cancer Res. 2007;5(11):1159–70.
56. Schachtschneider KM, Schwind RM, Darfour-Oduro KA, De AK, Rund LA, Singh K, Principe DR, Guzman G, Ray CE Jr, Ozer H, and others. A validated, transitional and translational porcine model of hepatocellular carcinoma. Oncotarget 2017;8(38):63620–34.